

# Electron attachment to molecules in a cluster environment

M. Smyth<sup>1</sup>, J. Kohanoff<sup>1</sup>, and I. I. Fabrikant<sup>2,3</sup> \*

<sup>1</sup> *Atomistic Simulation Centre, Queen's University Belfast,  
Belfast BT7 1NN, Northern Ireland, UK*

<sup>2</sup> *Department of Physics and Astronomy,  
University of Nebraska, Lincoln, Nebraska 68588, USA*

<sup>3</sup> *Department of Physical Sciences, The Open University,  
Walton Hall, Milton Keynes MK7 6AA, UK*

(Dated: February 6, 2014)

## Abstract

Low-energy electron-impact hydrogen loss due to dissociative electron attachment (DEA) to the uracil and thymine molecules in a water cluster environment is investigated theoretically. Only the  $A'$ -resonance contribution, describing the near-threshold behavior of DEA, is incorporated. Calculations are based on the nonlocal complex potential theory and the multiple scattering theory, and are performed for a model target with basic properties of uracil and thymine, surrounded by five water molecules. The DEA cross section is strongly enhanced when the attaching molecule is embedded in a water cluster. This growth is due to two effects: the increase of the resonance lifetime and the negative shift in the resonance position due to interaction of the intermediate negative ion with the surrounding water molecules. A similar effect was earlier found in DEA to chlorofluorocarbons.

PACS numbers: PACS No. 34.80.Ht, 31.70.Dk, 36.40.Mr

---

\* e-mail: ifabrikant1@unl.edu

## I. INTRODUCTION

Exposure of living cells to ionizing radiation leads to biological damage by both direct and indirect interaction with the cell components. During the last decade there has been increasingly stronger evidence that secondary electrons with energies below 20 eV have the capability of producing single and double strand breaks in DNA [1–5]. The exact mechanism of these strand breaks is still under discussion, but it is becoming more apparent that dissociative electron attachment (DEA) processes are playing a decisive role in this damage.

The most abundant product of DEA to the building blocks (purines and pyrimidines) of DNA is the dehydrogenated closed-shell anion  $[M-H]^-$  [6], therefore a lot of effort was devoted to studies of the hydrogen loss due to DEA to uracil and DNA bases [5, 7–15]. A series of sharp peaks in DEA cross sections to uracil [7–13], thymine [14], and adenine [12] were identified as vibrational Feshbach resonances (VFRs) [16]. The lowest  $A'$  anion state is strongly antibonding between N1 and H, where the number 1 refers to the atom location, see Fig. 1, and drives low-energy DEA with the production of a  $(U-H)^-$  anion and a H atom. In addition, due to the large dipole moment of uracil, the incident electron can be captured in the dipolar field with simultaneous vibrational excitation leading to VFR. The thymine molecule is not different in this regard, and the same mechanism is working in N1-H bond breaking in thymine at the energy of about 1 eV. As was shown by Ptasinka *et al.*, [12], there is a second peak in the H production at about 2 eV for both targets which is due to breaking the N3-H bond. The first peak was described quantitatively by Gallup and Fabrikant [17] by the use of a combination of the finite-element discrete model [18] with the resonance R-matrix theory [19].

In biological systems, it is important to know how these fundamental mechanisms are affected and modified in the presence of vital cellular components, in particular water [5]. First-principles molecular dynamics simulations [20] indicate that the excess electron in solvated DNA bases, although initially delocalized, localizes around the nucleobases within a 15 fs time scale. At this stage electrons exist in the so-called presolvated (or prehydrated) state [21, 22], and DEA processes might be strongly enhanced. In particular Lu and Sanche showed that due to its strong trapping properties,  $H_2O$  ice strongly enhances DEA processes in halocarbons [21] and hydrogen halides [22]. The DEA of electrons trapped in ice to chlorofluorocarbons plays an important role in the ozone-depletion chemistry in polar

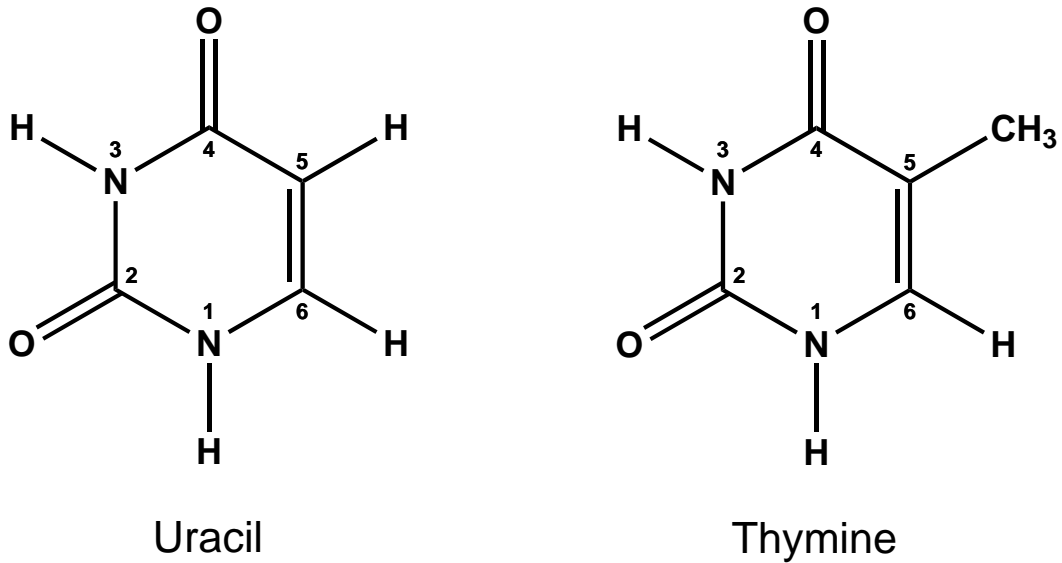


FIG. 1: Structure of uracil and thymine ring. Numbers by the chemical symbols indicate the atom positions. In this paper we discuss the N-H bond breaking at the N1 position.

stratospheric clouds [23, 24]. Similar effects were observed in biological systems [25, 26] revealing a new mechanism for reductive DNA damage.

The effect of DEA enhancement for chlorofluorocarbons in a water cluster environment was recently described quantitatively [27] by combining multiple-scattering theory [28–30] with the resonance R-matrix theory [19]. The calculations confirmed the existence of a strong enhancement in DEA due to the water cluster environment. This was interpreted in terms of electron trapping leading to a longer lifetime of the temporary negative-ion state and an increase of its survival probability.

In the present paper we extend our approach to electron attachment to uracil (U) and thymine (T) leading to hydrogen loss according to



From the point of view of our theoretical model there is no difference between U and T, and indeed, the experimental data [12] on DEA to uracil and thymine leading to breaking of the N1-H bond demonstrate very similar results. Therefore we assume that our results can be applied to both molecules and refer to the molecule under study as U/T.

First, we perform density functional calculations to establish the electronic and geometric structure of thymine embedded into a cluster of five water molecules. Then we employ the

resonance R-matrix method [19] to obtain scattering T-matrices for elastic  $e$ -U/T collisions. We incorporate these T-matrices, and T-matrices for scattering by water [30], in an extended multiple-scattering theory to include elastic electron scattering by the water molecules and attaching molecule. Finally, we carry out DEA calculations and compare the cross section for DEA to the isolated U/T molecule with that for the molecule surrounded by a water cluster. As in Ref. [17], we focus on the contribution of the lowest  $A'$  resonance leading to the first peak in the DEA cross section in the U/T system. The complete treatment of the problem requires inclusion of the coupling of  $A'$  with the second  $A''$  resonance [17]. This is much more challenging task which is postponed for future studies.

## II. T-(H<sub>2</sub>O) ELECTRONIC AND GEOMETRIC STRUCTURE

All electronic structure calculations were carried out using the computational package NWChem [31]. Geometry optimizations were performed at the density functional level of theory (DFT), using the hybrid functional PBE0 [32]. A triple-zeta basis supplemented with diffuse and polarization functions (6-311++G\*\*) was used. MP2 single-point energy calculations were performed at the optimized geometries using the aug-cc-pvtz basis set, in order to confirm the DFT results. The geometry of the cluster, as illustrated in Fig. 2 was extracted from a condensed phase model (described in [20]) and subsequently reoptimized. It is suggested that this system is representative of a liquid phase, where the five water molecules included are all within 3 Å of the thymine molecule and have thus formed hydrogen bonds with it. Indeed it has previously been suggested [33], and confirmed by us [20], that some of these H-bonds play an essential role in the stabilization of an excess electron in U/T. Note that, depending on the geometry of the complex, the water molecules can play a stabilizing or destabilizing role [34].

To find out how the presence of the water molecules affects the energy of the T<sup>-</sup> resonance states, we have calculated the vertical attachment energy (VAE), i.e. the energy difference between the anionic and neutral thymine molecule optimized in the neutral geometry. In Thymine there are two types of binding sites for the water molecules, proton acceptor (the oxygen atoms) and donor (the hydrogen atoms attached to the nitrogens in the ring). In our previous study [20] we showed that the adiabatic electron affinity (AEA) is more strongly affected by water binding to acceptor sites, while binding to donor sites has a detrimental

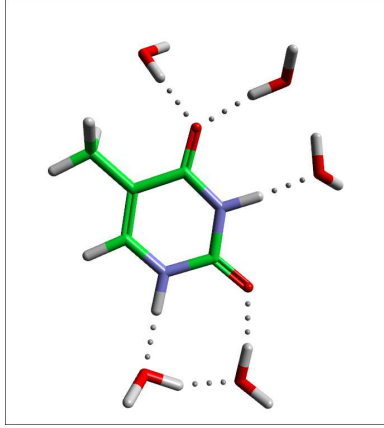


FIG. 2: Illustration of molecular structure of a fully optimized cluster, consisting of one thymine surrounded by five water molecules. The grey balls show hydrogen bonds within the structure.

effect. This same trend is observed here for the VAE. Therefore, in order to examine the effect of the individual acceptor hydrogen bonds, we optimized the geometry of each one of the water molecules at their respective binding sites (Fig. 3). Table I shows the VAE for each case. Clearly, the binding of a single water molecule has a positive influence in the attachment of an excess electron, i.e. it lowers the VAE. The gas phase value of VAE for the lowest resonance state is 0.435 eV, which is in good agreement with experimental data [35] and scattering calculations [36] of the position of the first resonance of the  $A''$  symmetry. Upon addition of a single water molecule the VAE decreases to a value that ranges from 0.163 to 0.299 eV, depending on the location and characteristics of the H-bond (see Fig. 3). Finally, Table I reports also the VAE for a cluster consisting of thymine surrounded by the five water molecules, i.e. a fully solvated shell. The VAE decreases to 0.109 eV. We conclude that the first solvation shell leads to a negative shift of the resonance position of about  $-0.326$  eV. This shift should not depend substantially on the resonance symmetry, therefore we adopt this value for DEA calculations via the resonance of the  $A'$  symmetry. Additional solvation shells would further decrease the VAE, as shown in [20] for the AEA.

### III. ELASTIC $e$ -U SCATTERING

Low-energy electron collisions with uracil were studied theoretically using a range of different *ab initio* methods including the single-center expansion method [37, 38], Schwinger

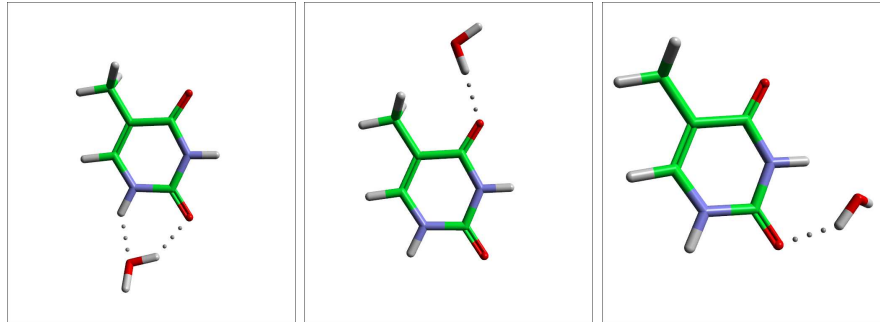


FIG. 3: Optimized structure of each individual water molecule attached to a thymine nucleobase, in configurations A, B and C, from left to right.

TABLE I: Vertical attachment energies for gas phase thymine, three thymine-single water structures (A, B and C), and the fully solvated cluster is also given (T+5H<sub>2</sub>O). Energies are calculated using PBE0 and 6-311++G\*\* basis set, and are given in eV.

U/T	1A	1B	1C	5H <sub>2</sub> O
0.435	0.299	0.163	0.218	0.109

variational method [36] and the R-matrix method [39]. These studies were focused on identification of narrow low-energy resonances, mainly of the  $A''$  (or  $\pi^*$ ) type that do not contribute directly to the low-energy DEA process because of their antisymmetric (with respect to the molecular plane) character. In contrast, the  $A'$  resonance is symmetric with respect to the molecular plane and contributes directly to DEA. In spite of its very large width, this resonance makes the major contribution in low-energy DEA in formic acid [40, 41], uracil [6, 13, 17] and aminobutanoic acid [42].

Since we are concentrating on the  $A'$  resonance contribution, our task is to perform a simple calculation of scattering matrices in the  $A'$  symmetry to be used in the multiple scattering theory of DEA. For the sake of consistency we employ the same resonance R-matrix model which was used in DEA calculations for uracil [17]. This model turned out to be successful for the description of low-energy electron scattering by simple polyatomic molecules [43]. A detailed description is given in Ref. [43]. Briefly, we start with the dipolar angular harmonics representation [44] for the S matrix. The lowest element  $S_{00}$  is calculated using the resonance R-matrix theory [19] with R-matrix parameters obtained from the finite-element-discrete-model calculations [17], and for all other elements the effective range theory

for electron scattering by polar molecules [45] is used. In this approximation the S matrix is diagonal in the projection of angular momentum quantum number  $m$ . Then the S matrix is transformed from the dipolar angular harmonics representation to the angular momentum representation and the partial in  $m$  cross sections  $\sigma^{(m)}$  are calculated.

In Fig. 4 we present the contribution of partial sums

$$\sigma_{\text{partial}} = \sum_{m=0}^{m_{\text{max}}} \sigma^{(m)} \quad (2)$$

for  $m_{\text{max}} = 3$  and  $m_{\text{max}} = 10$  to the elastic cross section in the  $A'$  symmetry. Note that, for higher  $m$ ,  $\sigma^{(m)}$  is well represented by the equation [45]

$$\sigma^{(m)} = \frac{4\pi\mu^2}{k^2} [2m^2\psi'(m) - 2m - 1]$$

where  $\psi'(m)$  is the derivative of the digamma function,  $\mu$  is the dipole moment, and  $k^2 = 2E$ ,  $E$  being the electron energy.

The total cross section in the fixed-nuclei approximation is divergent as harmonic series, and inclusion of molecular rotations is required to obtain a finite result that is not the purpose of the present work. We just note that qualitatively and semiquantitatively our  $\sigma_{\text{partial}}$  agrees with the results of *ab initio* calculations [36], although for a quantitative comparison it is necessary to know what is the effective cut-off in  $l$  and  $m$  in these calculations.

We also present the product  $\sigma^{(0)}E$  to show the influence of the  $\sigma^*$  resonance on the elastic cross section. Since the resonance is very broad this influence is hardly noticeable. Therefore, it is not surprising that the resonance was not detected in the *ab initio* calculations [36, 37, 39], although Winstead and McKoy [36] state that “it is possible that weak and/or broad  $\sigma^*$  resonances could be hidden in the very large nonresonant  $A'$  background.” Gianturco *et al* [38] observed a similar trend. This resonance is stabilized quickly with the stretching of the N1-H bond [17], and this is what makes it important for our DEA calculations.

The T-matrices for electron scattering by the water molecule were obtained by *ab initio* R-matrix calculations as discussed in Refs. [27, 29, 30].

#### IV. MULTIPLE SCATTERING THEORY

In Ref. [27] we applied the multiple-scattering theory [28–30] to calculations of attachment amplitude in the presence of a water cluster. The expressions we used incorporated

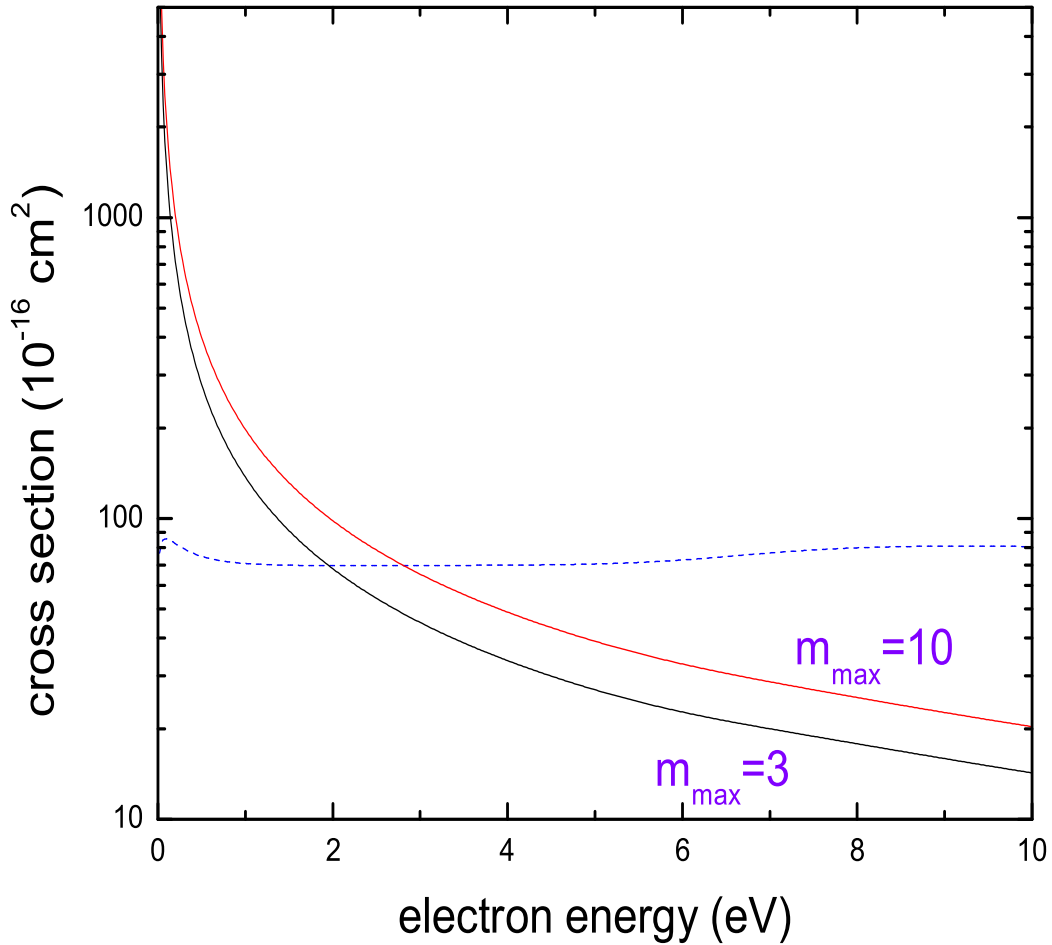


FIG. 4: Partial sums, Eq. (2), for  $m_{\max} = 3$  and 10. Blue dashed line: The product  $\sigma^{(0)}E$  in units  $10^{-16} \text{ cm}^2 \cdot \text{eV}$ .

multiple scattering effects only partially, since they did not include elastic scattering by the attaching molecule. Here we remove this deficiency by incorporating all scattering events.

To find the attachment amplitude, we will follow the approach of Caron and Sanche [28], but use a somewhat different notation, more convenient for our problem, whereby only one molecule (U/T) captures the electron while others (the water molecules) act as rescatterers. In contrast, Caron and Sanche assume that each molecule in the cluster captures electron with the same attachment probability.

In the spirit of multiple-scattering theory [46], we represent the field of the cluster by a potential consisting of two types of regions defined by a set of non-overlapping spheres centered on the individual molecules at their corresponding centers of mass. The potential within each sphere is equal to the potential (not necessarily spherically-symmetric) of the corresponding molecule, and we assume that the potential is zero outside the spheres. This condition restricts the number of partial waves involved in multiple scattering by the condition  $l \leq l_{\max} = kr_{\min}$  where  $r_{\min}$  is the minimum distance between molecular units in the cluster [29, 30]. This approach is approximate, of course, since it neglects the long-range part of the potential due to each molecular unit. It is reasonable to neglect these long-range effects within the cluster. However, outside the cluster these effects might be significant if the net dipole moment and/or polarizability of the cluster is significant. Therefore Dill and Dehmer [46] introduced a third region, outside the sphere of a larger radius, where the effects of the net dipole moment and polarizability can be included. These effects in scattering by water clusters were discussed by Caprasecca *et al.* [30]. Here we note that whereas these effects are important in elastic scattering, they should be insignificant in the electron attachment problem, since the resonance capture amplitude is dominated by a very few partial waves.

The asymptotic form of the wave function outside the sphere encompassing the molecule  $n$  is

$$\Psi(\mathbf{r}_n) = 2\pi i^l \sum_{LL'} A_L^n [2j_l(kr_n)\delta_{LL'} + T_{LL'}^n h_{l'}^{(1)}(kr_c)] Y_{L'}(\hat{\mathbf{r}}_n), \quad (3)$$

where  $\mathbf{r}_n$  is the electron position relative to the molecule  $n$ ,  $\mathbf{k}$  is the momentum of the incident electron,  $L = (l, m)$ ,  $j_l$  and  $h_l^{(1)}$  are spherical Bessel and Hankel functions, and  $T_{LL'}^n$  is the corresponding scattering matrix. The amplitudes  $A_L^n$  are determined from the system of linear equations

$$A_L^n(\mathbf{k}) = e^{i\mathbf{k}\cdot\mathbf{R}_n} Y_L^*(\hat{\mathbf{k}}) + \frac{1}{2} \sum_{n' \neq n} \sum_{L_1 L_2 L_2'} i^{l_2 - l} A_{L_2}^{n'}(\mathbf{k}) \tilde{F}_{mm_1 m_2'}^{l_1 l_2'} T_{L_2 L_2'}^{n'} h_{l_1}^{(1)}(R_{nn'}) Y_{L_1}(\hat{\mathbf{R}}_{nn'}) \quad (4)$$

where  $\mathbf{R}_n$  is the position of the center of mass relative to the origin,  $\mathbf{R}_{nn'} = \mathbf{R}_n - \mathbf{R}_{n'}$ , and

$$\tilde{F}_{m_1 m_2 m_3}^{l_1 l_2 l_3} = i^{l_1 + l_2 - l} (-1)^m [4\pi(2l_1 + 1)(2l_2 + 1)(2l_3 + 1)]^{1/2} \begin{pmatrix} l_1 & l_2 & l_3 \\ 0 & 0 & 0 \end{pmatrix} \begin{pmatrix} l_1 & l_2 & l_3 \\ m_1 & m_2 & m_3 \end{pmatrix}. \quad (5)$$

The  $\begin{pmatrix} \cdot & \cdot & \cdot \\ \cdot & \cdot & \cdot \end{pmatrix}$ s represent Wigner 3- $j$  symbols.

Eq. (4) contains all amplitudes including the amplitude  $A_L^c$  for the attaching molecule. After it is obtained, the capture amplitude  $V^{(c)}$  is calculated as

$$V^{(c)}(\mathbf{k}) = \sum_L A_L^c(\mathbf{k}) V_L^{(0)} \quad (6)$$

where  $V_L^{(0)}$  is the partial capture amplitude for an isolated molecule related to the total capture amplitude  $V^{(0)}(\mathbf{k})$  by the equation

$$V^{(0)}(\mathbf{k}) = \sum_L V_L^{(0)} Y_L^*(\hat{\mathbf{k}}). \quad (7)$$

The capture amplitude  $V^{(c)}(\mathbf{k})$  can be rewritten in the following form convenient for calculations

$$V^{(c)}(\mathbf{k}) = \sum_{nL} C_{nL} e^{i\mathbf{k}\cdot\mathbf{R}_n} Y_L^*(\hat{\mathbf{k}}) \quad (8)$$

where

$$C_{nL'} = \sum_L V_L^{(0)} (M^{-1})_{LL'}^{cn} \quad (9)$$

and the matrix  $M$  is given by

$$M_{LL'}^{nn'} = \delta_{LL'}^{nn'} - \frac{1}{2} (1 - \delta_{nn'}) i^{l'-l} \sum_{L_1 L_2} h_{l_1}^{(1)}(R_{nn'}) Y_{L_1}(\hat{\mathbf{R}}_{nn'}) \tilde{F}_{mm_1 m_2}^{ll_1 l_2} T_{L' L_2}^n. \quad (10)$$

Note that in the equations above the capture amplitude is dependent on internal nuclear coordinates  $q$ . Inclusion of this dependence is necessary for inclusion of nuclear motion during the DEA process. First we calculate the resonance width  $\Gamma(q, k)$  by performing the angular integration

$$\Gamma(q, k) = 2\pi \int |V^{(c)}(\mathbf{k}, q)|^2 d\hat{\mathbf{k}}. \quad (11)$$

For the calculation of the DEA cross section we solve an inhomogeneous Schrödinger equation with a nonlocal complex potential [47] which is constructed from the width function  $\Gamma(q)$  and the shift function

$$\Delta(q, k) = \frac{1}{2\pi} \text{P} \int_0^\infty dE' \frac{\Gamma(q, k')}{E - E'} \quad (12)$$

where  $E = k^2/2$ . The basic equation of the nonlocal complex potential theory is solved by the quasiclassical method as described in Refs. [48, 49]. So far this theory has been developed for a one-dimensional case only, that is, it assumes that a single vibrational coordinate dominates the dissociation path. The calculations presented in the present paper also assume the one-dimensional approximation.

## V. POTENTIAL ENERGY CURVES

The potential energy curves for the neutral molecule and the negative ions were taken from calculations for the isolated uracil [17] where the anion energy  $U$  as a function of the relative internuclear separation  $\rho$  was parametrized by the Morse potential

$$U(\rho) = Be^{-2\beta\rho} - Ce^{-\beta\rho} + D. \quad (13)$$

Since the resonance shift in the nonlocal complex potential theory, Eq. (12), is substantially different from the R-matrix resonant shift, our anion potential curve should be readjusted to obtain the same scattering cross section, in particular DEA cross sections. As a result of this readjustment, we obtained the following values of the Morse parameters (all numbers are in a.u.):  $B = 0.0228$ ,  $C = -0.1137$ ,  $D = 0.007$ .

We assume that the presence of the water molecules does not change the energy of the neutral uracil. However, as is well known, the energy of the anion is very sensitive to the environment. In particular, the dipolar and polarization forces from the water molecule can cause a substantial shift in the position of the anion curve. As a first step towards inclusion of this effect, we use the shift in the position of the lowest resonance of the  $A''$  symmetry as described in Sec. II.

## VI. RESULTS AND DISCUSSION

The DEA cross sections, calculated according to the discussed model, describe the  $\sigma^*$  (or  $A'$ )-resonance contribution to the hydrogen loss at the position N1 in reaction (1). At higher energies the hydrogen loss at the N3 site due to vibronic coupling between  $\sigma^*$  and the second  $\pi^*$  (or  $A''$ ) resonance is important [11], therefore the calculated cross section is substantially lower than the measured total H loss [12]. In addition, the position of the first peak in DEA cross section, below the excitation threshold of the N1-H( $\nu = 3$ ) vibration,  $E_{peak} = 1.2$  eV is higher than the observed peak [11, 12] by about 0.2 eV. These disagreements were discussed in Ref. [17]. In the present paper we do not attempt to improve the agreement with experiment, rather we employ the model constructed in Ref. [17] to study the effect of surrounding water molecules on the DEA cross sections.

In Fig. 5 we present the effect of multiple scattering on the resonance width as a function

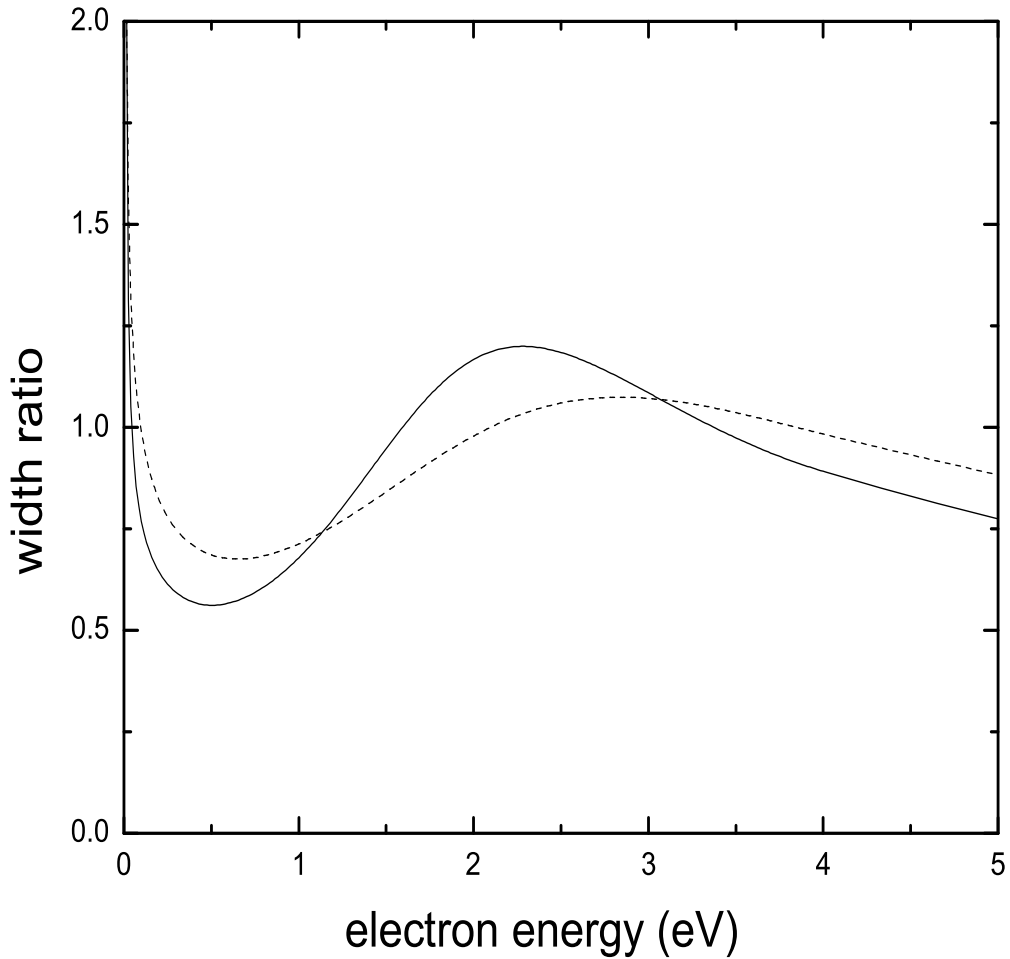


FIG. 5: The ratio of resonance widths, Eq. (14), as a function of energy calculated for the equilibrium internuclear separation. Solid curve, with inclusion of scattering by all molecules in the  $(\text{H}_2\text{O})_5$  cluster. Dashed curve, with inclusion of scattering by only water molecules.

of energy for the U/T molecule for a fixed nuclear geometry expressed in terms of the ratio

$$R(q, E) = \frac{\Gamma_{cl}(q, E)}{\Gamma_{mol}(q, E)} \quad (14)$$

where  $\Gamma_{mol}$  is the width for the isolated molecule, and  $\Gamma_{cl}$  that for the cluster. This ratio is almost independent of the internuclear separation  $q$ .  $\Gamma_{mol}$  was obtained earlier in Ref. [17] Since the width on the whole positive energy axis is necessary to obtain the resonance shift

according to Eq. (12), we extend both  $\Gamma_{mol}$  and  $\Gamma_{cl}$  by a smooth continuation in the region  $E > E_0 = 5$  eV using the function

$$\Gamma = \Gamma(E_0) \exp[-\alpha(E - E_0)^2] \quad (15)$$

for  $E > E_0$  [47].

The width for the U/T-(H<sub>2</sub>O)<sub>5</sub> system is smaller than for the isolated U/T almost in the whole energy range except in the narrow low-energy region and the region in the vicinity of  $E = 2$  eV. The effect is not as drastic as was previously found for chlorofluorocarbons embedded in water clusters [27], but significant, particularly in the low-energy region. Note that the width is significantly reduced at energies between 0.1 and 1 eV. We interpret this width reduction as the increase of the resonance lifetime due to the electron trapping in the water cluster environment [27]. For the DEA process this should lead to a substantial variation of the DEA cross sections. We should note, however, that the threshold behavior of cross sections is also strongly influenced by the net dipole moment of the system, and this is not included in the present calculations.

Based on the results for the width reduction, we expect higher survival probability for the intermediate anion state and higher DEA cross sections. In addition, the negative shift of the potential energy curve (referred below as the negative shift effect) should lead to a further increase of DEA cross sections.

In Fig. 6 we present DEA cross sections. In order to separate the multiple scattering effect from the negative shift effect, we present the cross sections for three values of the shift, +0.04, 0 and -0.04 eV. The result for the calculated value of the shift, -0.326 eV, is presented in Fig. 7. We observe that the multiple scattering effect increases the DEA cross section by about a factor of 2 (red dashed vs. black solid line in Fig. 6), but the most dramatic change occurs due to the negative shift effect. The slightly shifted calculations presented in Fig. 6 (blue, red, and green dashed lines) already show quite a clear trend, but when the full shift of -0.326 eV is applied as in Fig. 7, it results in a factor of 6 increase of the DEA cross section to U/T in the water cluster environment as compared to that for the isolated molecule. In addition, the position of the peak in the DEA cross section moves substantially towards lower energies. This effect is similar to that observed in DEA to methyl iodide clusters [50] and physisorbed molecules [51].

To analyze the influence of allowing for scattering also by the U/T molecule, apart from

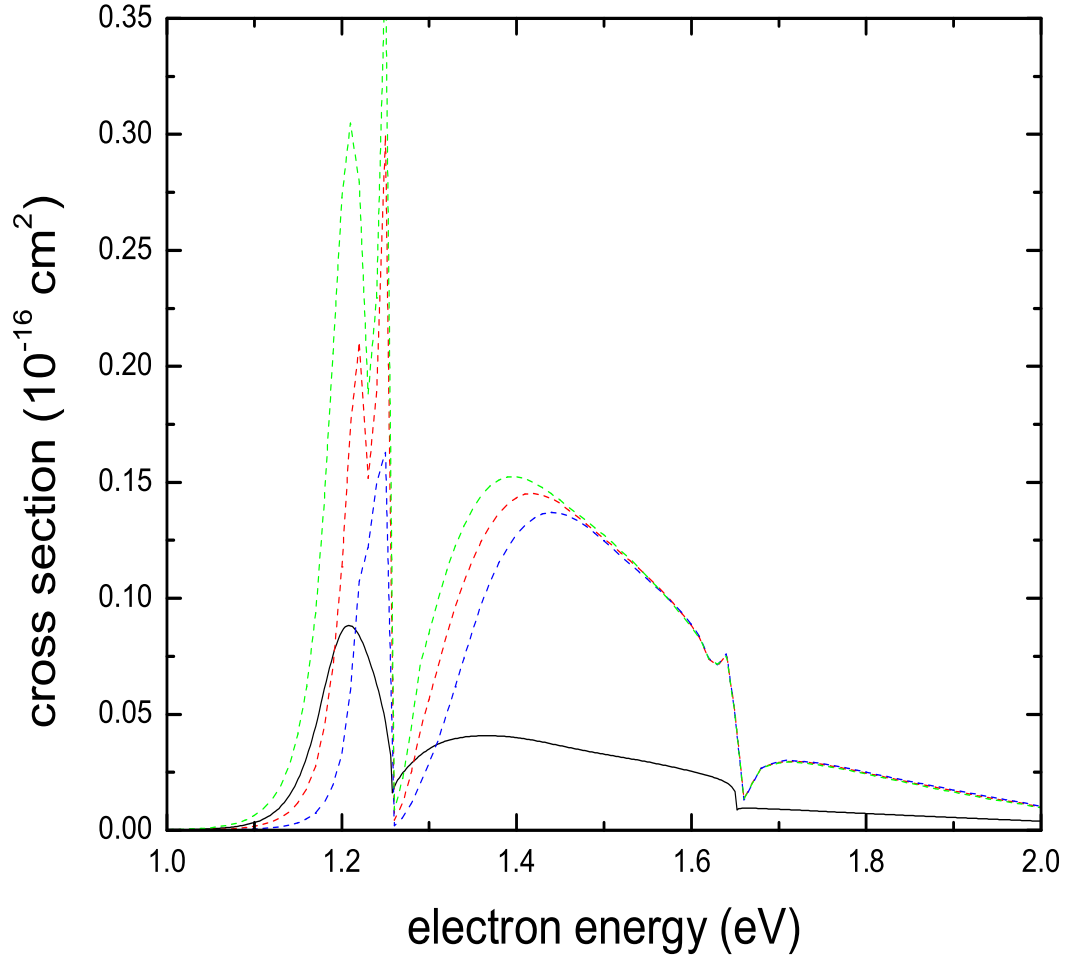


FIG. 6: Dissociative attachment cross section for isolated U/T (black solid curve) and for U/T embedded in the  $(\text{H}_2\text{O})_5$  cluster calculated for three values of the VAE shift  $\Delta E$  (dashed curves from bottom to top): blue,  $\Delta E = 0.04$  eV; red,  $\Delta E = 0$ ; green,  $\Delta E = -0.04$  eV.

the waters, we also present in Fig. 7 the cross section calculated in its absence. The cross section is affected slightly, but threshold structures change significantly. This is not surprising in view of the differences in the low-energy behavior of the width ratio  $R$ , Eq. (14).

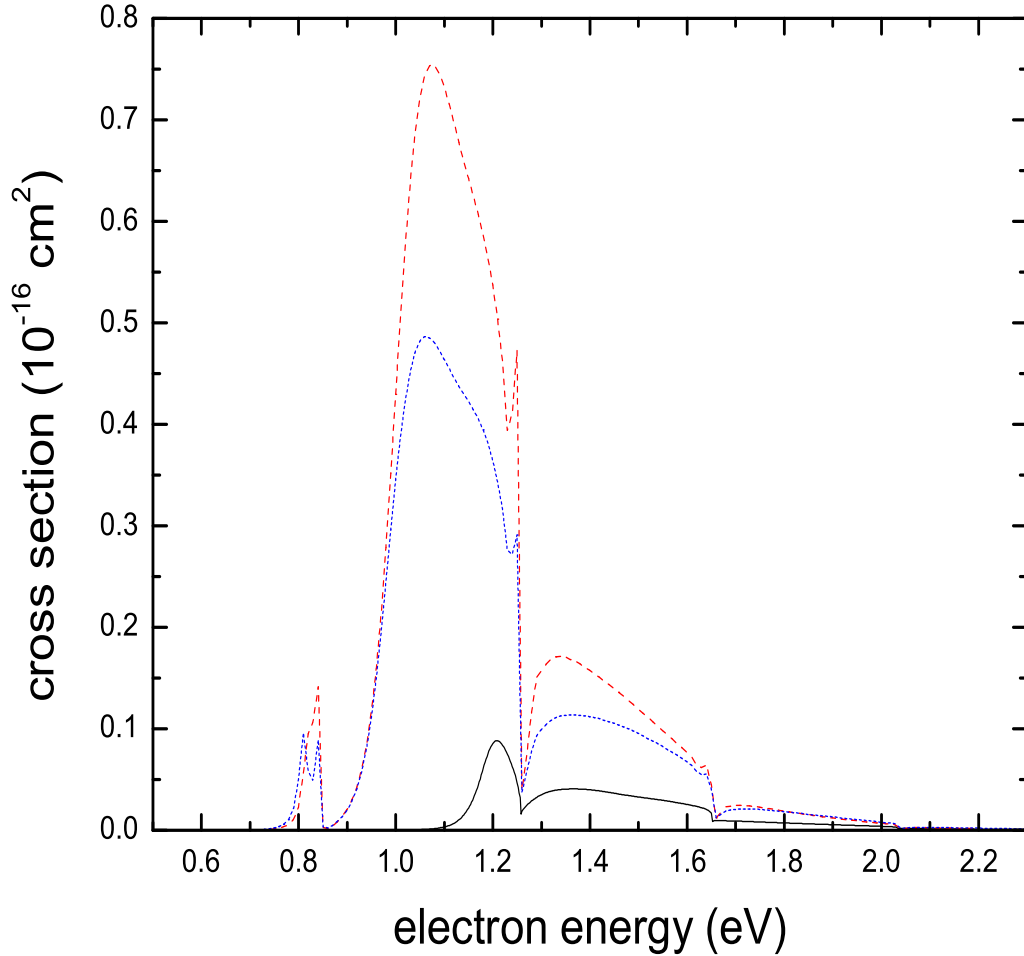


FIG. 7: Dissociative attachment cross section for isolated U/T (solid curve) and U/T embedded in the  $(\text{H}_2\text{O})_5$  cluster with VAE shift  $\Delta E = -0.326$  eV. Dashed red curve, with inclusion of scattering by all molecules in the  $(\text{H}_2\text{O})_5$  cluster. Short-dashed blue curve, with inclusion of scattering by only water molecules.

## VII. CONCLUSION

The approach used in the present paper allows us to study several interesting effects in DEA to the U/T molecule in a cluster environment. We confirm our previous observation [27] that placing an attaching molecule in a water cluster reduces the resonance width

and increases DEA cross sections. In addition, elastic electron scattering by the attaching molecule can influence the DEA process as well. Because of the restrictions on the orbital angular momenta involved in multiple scattering, it is unlikely that resonances dominated by higher angular momenta (like  $\pi^*$ ) contribute to DEA processes in a cluster environment.

On the other hand, the cut-off in  $l$  procedure is approximate itself, and might miss some features in the capture amplitude. More research with regard to convergence in  $l_{\max}$  is necessary. It is also important to have experimental data for DEA in “clear” systems, containing U/T in a well-defined water cluster. Presently such data do not exist, and we hope that the present paper will stimulate experimental studies in this direction.

An interesting question arises from the present studies. In the gas phase the hydrogen lost due to DEA will fly away and be collected in the mass spectrometer. In the condensed phase environment, the cleaved hydrogen will find a dense medium of water molecules and, by colliding with these molecules, it may not necessarily move very far away from U/T. It is then possible for this H atom to bind again to  $(\text{T-H})^-$ , while the excess energy is thermally dissipated in the water environment. The binding energy of an H atom to a water molecule is extremely small, so that the dehydrogenated anion remains the most attractive possibility. First-principles molecular dynamics simulations are currently underway in order to assess the fate of the lost hydrogen.

### Acknowledgments

The authors thank J. Gorfinkiel and Z. Mašín for useful discussions, and M. Ferguson for help in creating Fig. 1. IIF was supported by the Open University’s CEPSAR Research Centre as a visiting professor, and by the US National Science Foundation, Grant No. PHY-0969381. The electronic structure calculations were carried out in the HECToR Supercomputing Facility at Daresbury through EPSRC grant EP/K013459/1, allocated to the UKCP Consortium.

- 
- [1] B. Boudaiffa, P. Cloutier, D. Hunting, M. A. Huels, and L. Sanche, *Science* **287**, 1658 (2000).
  - [2] L. Sanche, *Eur. Phys. J. D* **35**, 367 (2005).
  - [3] R. Barrios, P. Skurski, and J. Simons, *J. Phys. Chem. B* **106**, 7991 (2002).

- [4] X. F. Li, M. D. Sevilla, and L. Sanche, *J. Am. Chem. Soc.* **125**, 13668 (2003).
- [5] S. Ptasinska and L. Sanche, *Phys. Rev. E* **75**, 031915 (2007).
- [6] S. Denifl, P. Sulzer, F. Zappa, S. Moser, B. Kräutler, O. Echt, D. K. Bohme, T. D. Märk, and P. Scheier, *Int. J. Mass Spectrom.* **277**, 296 (2008).
- [7] G. Hanel, B. Gstir, S. Denifl, P. Scheier, M. Probst, B. Farizon, M. Farizon, E. Illenberger, and T. D. Märk, *Phys. Rev. Lett.* **90**, 188104 (2003).
- [8] A. M. Scheer, K. Aflatooni, G. A. Gallup, and P. D. Burrow, *Phys. Rev. Lett.* **92**, 068102 (2004).
- [9] S. Feil, K. Gluch, S. Matt-Leubner, P. Scheier, J. Limtrakul, M. Probst, H. Deutsch, K. Becker, A. Stamatovic, and T. D. Märk, *J. Phys. B* **37**, 3013 (2005).
- [10] K. Aflatooni, A. M. Scheer, and P. D. Burrow, *Chem. Phys. Lett.* **408**, 426 (2005).
- [11] A. M. Scheer, C. Silvernail, J. A. Belot, K. Aflatooni, G. A. Gallup, and P. D. Burrow, *Chem. Phys. Lett.* **411**, 46 (2005).
- [12] S. Ptasinska, S. Denifl, P. Scheier, E. Illenberger, and T.D. Märk, *Angew. Chem. Int. Ed.* **44**, 6941 (2005).
- [13] P. D. Burrow, G. A. Gallup, A. M. Scheer, S. Denifl, S. Ptasinska, T. Märk, and P. Scheier, *J. Chem. Phys.* **124**, 124310 (2006).
- [14] S. Denifl, S. Ptasinska, M. Probst, J. Hrusak, P. Scheier, and T. D. Märk, *J. Phys. Chem. A* **108**, 6562 (2004).
- [15] H. D. Flosadottir, S. Denifl, F. Zappa, N. Wendt, A. Mauracher, A. Bacher, H. Johnsson, T. D. Märk, P. Scheier, and O. Ingolfsson, *Angew. Chem. Int. Ed.* **46**, 8057 (2007).
- [16] H. Hotop, M.-W. Ruf, M. Allan, and I. I. Fabrikant, *Adv. At. Mol. Phys.* **49**, 85 (2003).
- [17] G. A. Gallup and I. I. Fabrikant, *Phys. Rev. A* **83**, 012706 (2011).
- [18] R. K. Nesbet, *Phys. Rev. A* **24**, 1184 (1981).
- [19] I. I. Fabrikant, *Phys. Rev. A* **43**, 3478 (1991).
- [20] M. Smyth and J. Kohanoff, *Phys. Rev. Lett.* **106**, 238108 (2011).
- [21] Q.-B. Lu and L. Sanche, *Phys. Rev. B* **63**, 153403 (2001).
- [22] Q.-B. Lu and L. Sanche, *J. Chem. Phys.* **115**, 5711 (2001).
- [23] Q.-B. Lu and L. Sanche, *Phys. Rev. Lett.* **87**, 078501 (2001).
- [24] H. Tachikawa, *PCCP* **10**, 2200 (2008).
- [25] C.-R. Wang, J. Nguyen, and Q.-B. Lu, *J. Am. Chem. Soc.* **131**, 11320 (2009).

- [26] J. Nguyen, Y. Ma, T. Luo, R. G. Bristow, D. A. Jaffray, and Q.-B. Lu, PNAS **108**, 11778 (2011).
- [27] I. I. Fabrikant, S. Caprasecca, G. A. Gallup, and J. D. Gorfinkiel, J. Chem. Phys. **136**, 184301 (2012).
- [28] L. G. Caron and L. Sanche, Phys. Rev. Lett. **91**, 113201 (2003).
- [29] D. Bouchiha, L. G. Caron, J. D. Gorfinkiel and L. Sanche, J. Phys. B **41**, 045204 (2008).
- [30] S. Caprasecca, J. D. Gorfinkiel, D. Bouchiha, and L. G. Caron, J. Phys. B **42**, 095205 (2009).
- [31] M. Valiev, E.J. Bylaska, N. Govind, K. Kowalski, T.P. Straatsma, H.J.J. van Dam, D. Wang, J. Nieplocha, E. Apra, T.L. Windus, W.A. de Jong, Comput. Phys. Commun. **181**, 1477 (2010).
- [32] C. Adamo and V. Barone., J. Chem. Phys. **110**, 6158 (1999).
- [33] S. Kim, S. E. Wheeler, and H. F. Schaefer, J. Chem. Phys. **124**, 204310 (2006).
- [34] T. C. Freitas, K. Coutinho, M. T. do N. Varella, M. A. P. Lima, S. Canuto, and M. H. F. Bettega, J. Chem. Phys. **138**, 174307 (2013).
- [35] K. Aflatooni, G. A. Gallup, and P. D. Burrow, J. Chem. Phys. A **102**, 6205 (1998).
- [36] C. Winstead and V. McKoy, J. Chem. Phys. **125**, 174304 (2006).
- [37] F. A. Gianturco and R. R. Lucchese, J. Chem. Phys. **120**, 7446 (2004).
- [38] F. A. Gianturco, F. Sebastianelli, R. R. Lucchese, I. Baccarelli and N. Sanna, J. Chem. Phys. **128**, 174302 (2008).
- [39] A. Dora, J. Tennyson, L. Bryjko and T. van Mourik, J. Chem. Phys. **130**, 164307 (2009).
- [40] G. A. Gallup, P. D. Burrow, and I. I. Fabrikant, Phys. Rev. A **79**, 042701 (2009)
- [41] R. Janečková, D. Kubala, O. May, J. Fedor, and M. Allan, Phys. Rev. Lett. **111**, 213201 (2013)
- [42] V. Vizcaino, B. Puschnigg, S. E. Huber, M. Probst, I. I. Fabrikant, G. A. Gallup, E. Illenberger, P. Scheier, and S. Denifl, New J. Phys. **14**, 043017 (2012)
- [43] G. A. Gallup and I. I. Fabrikant, Phys. Rev. A **75**, 032719 (2007).
- [44] M. H. Mittleman and R. E. von Holdt, Phys. Rev. **140**, A726 (1965).
- [45] I. I. Fabrikant, J. Phys. B **10**, 1761 (1977).
- [46] D. Dill and J. L. Dehmer, J. Chem. Phys. **61**, 692 (1974).
- [47] W. Domcke, Phys. Rep. **208**, 97 (1991).
- [48] S. A. Kalin and A. K. Kazansky, J. Phys. B **23**, 4377 (1990).

- [49] G. A. Gallup, Y. Xu and I. I. Fabrikant, *Phys. Rev. A* **57**, 2596 (1998).
- [50] J. M. Weber, I. I. Fabrikant, E. Leber, M.-W. Ruf, and H. Hotop, *Eur. Phys. J. D* **11**, 247 (2000).
- [51] K. Nagesha, I. I. Fabrikant and L. Sanche, *J. Chem. Phys.* **114**, 4934 (2001).